Densities of States of Paramagnetic Cu-Ni Alloys*

G. M. Stocks, R. W. Willams,† and J. S. Faulkner
Metals and Ceramics Division, Oak Ridge National Laboratory, Oak Ridge, Tennessee 37830
(Received 6 July 1971)

The densities of states of the near ideally substitutional random-alloy system Cu-Ni are calculated using the coherent-potential approximation for a range of concentrations of the constituents across the complete alloy diagram. It is shown that previous model calculations for Ni-rich paramagnetic Cu-Ni alloys using the coherent-potential approximation can be extended to alloys of arbitrary concentration if appropriate Cu and Ni potential functions are used. The results obtained are consistent with experimental photoemission and soft-x-ray emission profiles in so far as comparisons can be effected. The results indicate the limits of this simple nonmagnetic random-alloy theory for discussing the conventional low-temperature specific-heat data of these alloys. For Cu-rich alloys the results correspond to a split-band regime while for Ni-rich alloys the d bands associated with Cu and with Ni sites in the alloy overlap to a considerable extent. For all Cu-Ni alloys the rigid-band model and the virtual-crystal approximation are quite inappropriate.

I. INTRODUCTION

For a given crystal potential function, the one-electron states of a perfect metal or compound can now be evaluated to a very high degree of precision. The situation in respect to disordered systems, e.g., compositionally disordered binary alloys, is much more complex and the electronic states may only be calculated at certain levels of approximation. However the coherent-potential approximation or CPA introduced by Soven[1] is providing a valuable level of approximation in understanding the one-electron properties of disordered systems in general and disordered metallic alloys in particular. The CPA results from the self-consistent solution of the multiple-scattering equations for an approximation in which $N-1$ of the N scattering centers of the system are replaced by an effective medium and the total scattering from the Nth site is treated exactly. In the hierarchy of possible approximations[2-8] to the complete solution of the N-center problem, the CPA represents a realistic level of approximation at which calculations can be performed.

Calculations based on simple model alloy systems by Soven[1] and by Velický *et al.*[7] have demonstrated the utility of this approximation. A model useful for treating Ni-rich Cu-Ni alloys within the CPA framework has been discussed by Kirkpatrick, Velický, and Ehrenreich[9] (KVE) together with some indication of the properties of the densities-of-states functions for these alloys. In a preliminary report the present authors (SWF)[10] have shown that if care is taken in assigning the potential functions to be associated with Cu and with Ni sites in the alloy then the model of KVE is easily extended for discussing Cu-rich Cu-Ni alloys. Levin and Ehrenreich[11] have also used the CPA within the framework of a simple model to discuss the electronic states and optical properties of the Ag-Au alloy system. Stocks[12] has shown that with minor modifications to account for lattice-parameter changes that the above model yields satisfactory results for noble-metal-rich Ag-Pd and Cu-Pd alloys. Stroud and Ehrenreich[13] have also used the CPA to discuss the band structure of the semiconducting system Si-Ge.

From the point of view of comparison of experimental results with the predictions of some theoretical model of the densities of states in a particular alloy it has been conventional to use some greatly simplified theoretical model. Chief among these models have been the rigid-band model,[2] the virtual-crystal approximation,[3,4] and more recently the virtual-bound-state model.[5,6] The conceptual simplicity of the rigid-band model and the virtual-crystal approximation has led to their widespread use, although for many alloy systems they are quite inappropriate. In the rigid-band model it is assumed that the parent metals, and alloys of them, have the same distribution of energy states. These states are filled to a level appropriate to the electron-to-atom ratio z of the system in question. In the virtual-crystal approximation for a random AB alloy in which one can associate potential functions V_A and V_B with A and B sites, respectively, it is assumed that one may replace the random array of V_A and V_B potentials with an ordered array of potentials V_{alloy} given by $V_{\text{alloy}} = cV_A + (1-c)V_B$, c being the concentration of A atoms. This problem can then be solved using standard band-theoretical techniques.

Both the rigid-band model and the virtual-crystal approximation require that the impurity scattering potential $(V_B - V_A)$ be small. This is not generally the case for alloys of metals which have scattering

resonances in or near to the conduction band, e.g., the noble metals and the transition metals.

The virtual-bound-state model would be expected to be more appropriate to a transition-metal impurity in a noble-metal host. This model basically describes the energy states of a single transition-metal impurity in a free-electron gas, although it has been generalized to treat other cases in an approximate manner. Using this model it is possible to qualitatively account for the structure between the Cu d-band structure and the Fermi energy which occurs in photoemission spectra[14] for extremely Cu-rich Cu-Ni alloys as well as certain resistivity[15] and thermoelectric-power data.[16] Although this type of model is qualitatively successful for Cu-rich Cu-Ni it is not a very useful description when the impurity concentration becomes sufficiently large that the impurity-impurity interaction becomes significant.

For historical reasons mention should be made of the average t-matrix approximation proposed in various forms by Korringa[17] and Beeby.[18] Efforts to use this approximation on one-dimensional models[1,19] and three-dimensional problems[20,21] were unsuccessful, but many of the concepts introduced in this work were useful in the development of the CPA. For completeness mention should also be made of the pseudopotential approaches to the theory of alloys of Ziman[22] and others.[23,24] These approaches have been quite successful in illuminating the electronic properties of the alkali metals but their range of applicability is limited to simple metals.

Here we present a complete account of calculations of the densities of states of paramagnetic Cu-Ni alloys of arbitrary concentration using the CPA. These calculations are based on the model of KVE[9] and the potential functions used by SWF[10] to describe Cu and Ni sites in the alloys. They represent the first complete account of the densities of states for Cu-Ni alloys of arbitrary concentration within a single framework. It is shown that these theoretical predictions are consistent with the gross features of experimental photoemission data[14,25,26] and experimental soft-x-ray data,[27–29] data which are probably largely insensitive to the magnetic state of the alloy in question. These results also give an indication of the contribution to the low-temperature specific heat which can be obtained from a simple paramagnetic theory and point to large effects which result from the electron-phonon interaction, magnetic interactions, and clustering in these alloys.

Despite the necessary mathematical complication of the CPA the results obtained for the densities of states in Cu-Ni alloys present a conceptually simple picture. The density-of-states function for Cu is characterized by a fairly narrow (3-eV) high density-of-states d band superimposed on a broad low density-of-states sp band in which the Fermi energy lies. The top of the d band being some 2 eV below the Fermi energy. On the addition of small amounts of Ni the CPA predicts the formation of an impurity d subband of approximately Lorentzian shape midway between the Cu d bands and the Fermi energy, this behavior being consistent with the virtual-bound-state model.[14,26] On increasing the Ni concentration the impurity subband grows at the expense of the host subband. The impurity subband develops structure at Ni concentrations of approximately 40% and finally evolves into the d-band structure of Ni in which the Fermi energy lies. During this process the d bands of Cu change their position with respect to Fermi energy very little, merely becoming smaller and more structureless.

Section II of this paper comprises a brief review of the CPA and of the model used for these calculations. The form of the potential functions used to describe pure Cu, pure Ni, and hence the alloys is discussed in Sec. III. The results of the calculations are presented in Sec. IV together with some preliminary discussion. Section V comprises a discussion of the experimental photoemission, optical properties, soft-x-ray spectroscopy, and low-temperature specific-heat data in terms of the calculated densities of states of Sec. IV. Section VI contains some concluding remarks.

II. MODEL

The form of the CPA we will use in these calculations is in essence that of Kirkpatrick, Velický, and Ehrenreich,[9] the important features of which are indicated below. A more complete account of the CPA is contained in the work of Soven[1] and of Velický *et al.*[7]

The one-particle Green's function for a particular configuration of an alloy system having Hamiltonian H is defined through

$$G(z) = (z - H)^{-1} . \tag{1}$$

The configurational average $\langle G(z)\rangle$ of this Green's function contains the maximum information that can be obtained from a calculation which uses only statistical information about the system. In particular the electronic densities of states $\rho(E)$ is related to $\langle G\rangle$ through

$$\rho(E) = -(\pi N)^{-1} \operatorname{Im} \operatorname{Tr}\langle G(E + i0)\rangle . \tag{2}$$

The CPA results from the solution of the multiple-scattering equations for the alloy system in an approximation (the single-site approximation[7]) in which the true crystal is replaced by an effective medium in which the electron propagates, the medium being chosen such that replacing it by a true atom at a given site n produces no further

scattering on the average. If t_n is the local scattering operator for the site n then, in operator notation,

$$t_n = (v_n - \Sigma)[1 - \tilde{G}(v_n - \Sigma)]^{-1} \ , \tag{3}$$

where v_n is the true atomic potential, Σ is the coherent potential which characterizes the effective medium, and $\tilde{G}$ is the Green's function for the effective medium (i.e., the ordered array of Σ's).

The basic result of the CPA is that Σ should be found from the equation

$$\langle t_n(\Sigma) \rangle = 0 \ . \tag{4}$$

When (4) is satisfied, then, within the single-site approximation, $\tilde{G} = \langle G \rangle$. For a random AB alloy, (4) becomes simply

$$c t_A + (1 - c) t_B = 0 \ , \tag{5}$$

where c is the concentration of A atoms.

The apparent simplicity of Eqs. (3) and (4) is deceptive since they can only be solved for certain forms of the potential function v_n. Also they require knowledge of the potential function which is to be associated with the atomic species in the alloy. Because of the nearly ideal substitutional nature of the Cu-Ni alloy system it is reasonable to associate the band-theory neutral-atom potential functions of pure Cu and pure Ni with Cu and Ni sites in the alloy. This no-charge-transfer model is also indicated by the recent Mössbauer isomer-shift data of Love *et al.*[30] which indicates that the nuclear contact density at the Ni nucleus does not depend on the concentration of Cu.

The similarity between the s bands of Ni and Cu suggests that it is reasonable to assume that Cu, Ni, and alloys of them have a common s band which can then be treated in a model Hamiltonian framework in terms of orthogonalized plane waves (OPW's). It is then possible to focus attention on the effects of alloying on the tight-binding d bands which are present in the parent metals. These d bands may be treated in terms of five tight-binding d functions such that in a basis of atomic orbitals $|\mu n\rangle$ the d-d block of the model Hamiltonian takes the form

$$H_{dd} = \sum_n |\mu n\rangle \epsilon_{\mu n} \langle \mu n| + \sum_{n \neq n';\, \mu, \mu'} |\mu n\rangle t_{\mu n, \mu' n'} \langle \mu' n'| \ , \tag{6}$$

where $|\mu n\rangle$ represents an atomic d function centered on the site n and the index μ describes the d-orbital symmetry which is t_{2g} for $\mu = 1, 2, 3$ and e_g for $\mu = 4, 5$. For an AB alloy the $\epsilon_{\mu n}$ take on values $\epsilon_{\mu A}$ and $\epsilon_{\mu B}$ appropriate to A and to B sites, respectively. If it is assumed that the off-diagonal elements of Eq. (6) are translationally invariant and independent of concentration the effects of alloying result only from the randomness of the $\epsilon_{\mu n}$.

Defining

$$\epsilon_{\mu A} = \tfrac{1}{2} \delta_\mu \ , \quad \epsilon_{\mu B} = -\tfrac{1}{2} \delta_\mu \ , \quad \delta_\mu = \epsilon_{\mu A} - \epsilon_{\mu B} \ , \tag{7}$$

the dependence of δ_μ on the orbital symmetry is sufficiently small in Cu-Ni ($\sim 3\%$ of its magnitude) that it may be neglected. Since the model treats only the effects of diagonal randomness in Eq. (6) these effects are then determined by the magnitude of the single parameter δ.

The interpolation Hamiltonian which we use for the Cu-Ni alloy system is constructed in a basis of four OPW's and five tight-binding Bloch functions and for a pure metal is simply the one used in the Hodges and Ehrenreich[31-33] interpolation scheme. By applying the CPA to the full interpolation Hamiltonian it is possible to calculate the densities of states of e_g and of t_{2g} symmetry denoted as $\rho_E(E)$ and $\rho_T(E)$, respectively. The total density of states $\rho(E)$ is given by

$$\rho(E) = \rho_E(E) + \rho_T(E) + \rho_s(E) \ , \tag{8}$$

where $\rho_s(E)$ is the density of states for the OPW sp band. For example, for states of $e_g (\equiv E)$ symmetry, the analysis of KVE leads to

$$\Sigma_E = \langle \epsilon_E \rangle - (\epsilon_E^{\mathrm{Cu}} - \Sigma_E) F_E (\epsilon_E^{\mathrm{Ni}} - \Sigma_E) \ , \tag{9}$$

where

$$\langle \epsilon_E \rangle = c \epsilon_E^{\mathrm{Cu}} + (1 - c) \epsilon_E^{\mathrm{Ni}} \tag{10}$$

and

$$F_E = (2N)^{-1} \mathrm{Tr} P_E \tilde{G} P_E \ , \tag{11}$$

P_E being a projection operator which selects the subspace of e_g symmetry. The density of states of e_g symmetry is given by

$$\rho_E = -(\pi N)^{-1} \mathrm{Im}\, \mathrm{Tr} P_E \tilde{G}(E + i0) \ , \tag{12}$$

there being a corresponding set of equations for states of t_{2g} symmetry. Equation (9) and its counterpart of t_{2g} symmetry are coupled since F_E and F_T both depend on Σ_E and Σ_T through $\tilde{G}$. However KVE show how to uncouple these equations subject to

$$\Sigma_E \tilde{=} \epsilon_E \ , \quad \Sigma_T \tilde{=} \epsilon_T \ ,$$

which leads to the set of equations

$$F_E(z) = F_E^{\alpha,0}(z - \Sigma_E + \epsilon_E^\alpha) \ , \tag{13}$$

$$F_E^{\alpha,0} = \frac{1}{2} \int \frac{dE\, \rho_E^{\alpha,0}(E)}{z - E} \ , \tag{14}$$

$$\rho_E^\alpha(E) = -(2/\pi)\, \mathrm{Im} F_E^\alpha(E + i0) \ , \tag{15}$$

where α denotes either Cu or Ni and the zero refers to the pure-metal case. It is worth commenting on the validity of the above decoupling of Eq.

(9) and its counterpart of t_{2g} symmetry. Direct calculation shows that the condition $\Sigma_E \cong \epsilon_E$ and $\Sigma_T \cong \epsilon_T$ is not well satisfied near band edges and becomes less well satisfied as the magnitude of δ increases when Σ_E and Σ_T have large imaginary parts. This problem is worse for Cu-rich alloys but the present calculations reveal that the errors involved are only in the order of 0.01 Ry in the band edges and are therefore at a tolerable level within the framework of the KVE model.

In addition to the above densities-of-states functions partial densities of states of e_g and t_{2g} symmetry at Cu and at Ni sites ρ_E^{Cu}, ρ_T^{Cu}, ρ_E^{Ni}, ρ_T^{Ni}, and total d densities of states at Cu and Ni sites $\rho^{Cu} = \rho_E^{Cu} + \rho_T^{Cu}$ and $\rho^{Ni} = \rho_E^{Ni} + \rho_T^{Ni}$ may also be calculated. For example,

$$\rho_E^{Ni}(E) = -(\pi N)^{-1} \operatorname{Im} \operatorname{Tr} P_E^{Ni} \bar{G}(E + i0) , \tag{16}$$

where P_E^{Ni} selects the subspace of e_g symmetry about Ni sites. Following KVE Eq. (16) leads, in the single-site approximation, to

$$\rho_E^{Ni}(E) = -(2/\pi)(\epsilon_E^{Ni} - \epsilon_E^{Cu})^{-1} \operatorname{Im}[(\Sigma_E - \epsilon_E^{Cu}) F_E(E + i0)] . \tag{17}$$

It is clear that if δ and the $\rho_E^{\alpha,0}$ and $\rho_T^{\alpha,0}$ which appear in Eq. (14) are known then it is possible to calculate in a simple manner the alloy density of states and the various contributions to it using the above equations and their equivalents for states of t_{2g} symmetry. As is evident from Eq. (14) there is some freedom in the choice of which pure-metal densities of states the alloy calculations are to be based. In the following we make the obvious choice of basing the alloy calculation on pure-metal densities of states of the metal which is the majority component of the alloy. In actuality the densities-of-states functions for Cu and Ni are rather similar aside from the position of the d bands. Thus the qualitative nature of the results which we obtain in this paper do not depend upon the choice, although the apparent semiquantitative agreement with say photoemission data is to some extent a consequence of the above assignment. The similarity between densities of states of Cu and Ni is of course the justification for making the assumption that the effects of alloying can be described in terms of only the diagonal randomness of the $\epsilon_{\mu n}$.

III. SPECIFICATION OF CRYSTAL POTENTIALS AND CALCULATION OF PURE-METAL DENSITIES OF STATES

A. General

Within the framework of the model discussed in Sec. II, calculation of the densities of states of a particular Cu-Ni alloy requires (apart from c) only specification of the matrix elements of the interpolation Hamiltonian for pure Cu and pure Ni from which the pure-metal quantities $\rho_E^{Cu,0}$, $\rho_T^{Cu,0}$, ρ_s^{Cu}, and their counterparts for Ni together with δ which appear in the CPA equations may be calculated. However in order to choose the matrix elements of the pure-metal interpolation Hamiltonian in a physical manner it is useful to have a reliable energy-band calculation for the metal on which the interpolation-Hamiltonian matrix elements may be based. These matrix elements may then, if necessary, be modified within certain limits in order to more precisely predict certain experimental quantities. We have based the interpolation-Hamiltonian parameters used in these calculations on our own Korringa-Kohn-Rostocker[34,35] (KKR) band-theory calculations which in turn were based on muffin-tin–crystal potential functions generated by a superposition of atomic-charge densities. It was found unnecessary to modify the parameters involved in the matrix elements of the interpolation Hamiltonian when using the potential functions to be described, since the predictions of the band-theory calculations agree well with the available experimental observations.

The spherically symmetric Coulomb and exchange potentials used to describe pure Cu and paramagnetic Ni were obtained by a superposition of atomic-charge densities according to the Mattheiss[36] prescription. The atomic-charge densities were obtained from a version of the Herman-Skillman[37] Hartree-Fock-Slater atomic-structure program. The Latter[38] cut off was not used. The exchange potential was taken as the Slater[39] form

$$V_{ex} = -6[3\rho(r)/8\pi]^{1/3} \tag{18}$$

in the generation of both the atomic and crystal potentials. The constant of potential between the muffin-tin spheres was calculated by averaging the spherically symmetric potential between the muffin-tin sphere and the Wigner-Seitz sphere. The muffin-tin radius was set at half the nearest-neighbor distance.

The band-theory calculations were performed with a symmetrized[40] version of the KKR method[41] including terms in the expansions to $l_{max} = 4$ which leads to convergence of the eigenvalues to better than 0.001 Ry. The fitting of the parameters involved in the matrix elements of the Hodges-Ehrenreich interpolation Hamiltonian is a standard procedure; we have followed Hodges[33] excepting we have allowed for a full fifteen-parameter fit to the energy bands by including $W_{2'}$ in the set of eigenvalues over which the fit is made. This allows the parameters B_1, B_2, and B_3 (in the notation of Hodges) to be fitted unequivocally for the set of eigenvalues used. The s, t_{2g}, and e_g components of the densities of states for the pure metals were obtained over the energy range of interest in the

TABLE I. Energy levels for Cu and Ni in Ry. The Cu and Ni lattice parameters were taken as 6.8032 and 6.6321 a.u., respectively.

	Cu	Ni		Cu	Ni
Γ_1	0.0	0.0	L_1	0.284	0.343
$\Gamma_{25'}$	0.412	0.535	L_3	0.408	0.528
Γ_{12}	0.467	0.614	L_3	0.508	0.670
X_1	0.279	0.334	$L_{2'}$	0.596	0.618
X_3	0.318	0.398	L_1	0.954	1.119
X_2	0.505	0.667	K_4	0.476	0.624
X_5	0.519	0.685	$W_{2'}$	0.330	0.402
$X_{4'}$	0.801	0.846	E_F	0.674	0.680

form of a 96-column histogram. In forming the histogram the eigenvalues were interpolated for a 505 weighted $\vec{k}$-point integration mesh in $\frac{1}{48}$th of the Brillouin zone. A finer integration mesh could obviously have been used but we feel that the above procedure is commensurate with the accuracy of the interpolation fit to the original pure-metal energy bands and with the model of Cu-Ni alloys of Sec. II.

B. Nickel

The Ni-lattice parameter was taken to be 6.6321 a.u. The crystal potential was then generated for a starting atomic configuration of $(3d)^{9.4}(4s)^{0.6}$, since the distribution of electronic charge in metallic Ni appears to be simulated by using this atomic configuration in the generation of the crystal potential.[42,43] It is known that the positioning of the d bands is quite sensitive to the assumed starting atomic configuration,[42-45] thus it is necessary to base the crystal potential on an atomic configuration which will reasonably approximate the self-consistent arrangement.

Eigenvalues obtained for this potential function for the set required for use in the interpolation scheme parametrization of the energy bands are shown in Table I. Fitting of these eigenvalues yields the interpolation-Hamiltonian parameters shown in Table II.

Figure 1 shows the total density of states (solid line) together with t_{2g} (short dash) and e_g (dotted) components of the total densities of states for the present Ni potential as calculated from the interpolation Hamiltonian and the $\vec{k}$-integration mesh discussed earlier. These are the Ni densities of states which are used in all subsequent calculations. The theoretical density of states is drawn such that the zero of energy is the calculated Fermi energy. This procedure is adopted for all calculated density of states curves which appear in this paper. Also shown in Fig. 1 are the optical densities-of-states results obtained from the photoemission experiments of Seib and Spicer[25] (medium dashed) and Eastman and Krolikowski[46] (long dashed). The experimental curves have been drawn such that the high-energy peak in the ODS curves coincides with the position of the upper sharp peak in the calculated density-of-states curve. The Fermi energy is marked E_F on each curve. Structure in the theoretical densities of states correlates well with structure in the optical densities of states of Eastman and Krolikowski, this perhaps being the more reliable of the two experiments.

There have been several attempts to construct an energy-band picture which will adequately describe nonmagnetic and ferromagnetic Ni, these being of both a first-principles and of an interpola-

TABLE II. Hodges-Ehrenreich interpolation scheme parameters for Cu and Ni.

Parameter	(a) Ni (Present)	(b) Ni (Hanus)	(c) Ni (Zornberg)	(d) Cu (Present)	(e) Cu (Burdick)
E_0	0.5760	0.5098	0.585	0.4418	0.4308
Δ	−0.0067	−0.0230	0.000	−0.0025	−0.0044
A_1	0.0273	0.0328	0.029	0.0192	0.0203
A_2	0.0086	0.0090	0.009	0.0059	0.0062
A_3	0.0133	0.0131	0.009	0.0087	0.0102
A_4	0.0179	0.0209	0.017	0.0117	0.0129
A_5	0.0034	0.0041	0.003	0.0024	0.0026
A_6	0.0113	0.0123	0.014	0.0082	0.0083
α	0.0168	0.0166		0.0152	0.0153
β	0.0000	0.0000	0.000	0.0000	0.0000
V_{111}	0.1872	0.1871		0.1346	0.1251
V_{200}	0.2281	0.2385		0.1731	0.1761
B_1	0.4670	0.4430		0.4620	0.4520
B_2	1.1492	1.2662		0.9106	0.9071
B_3	1.3363	1.1744		1.0572	1.0169

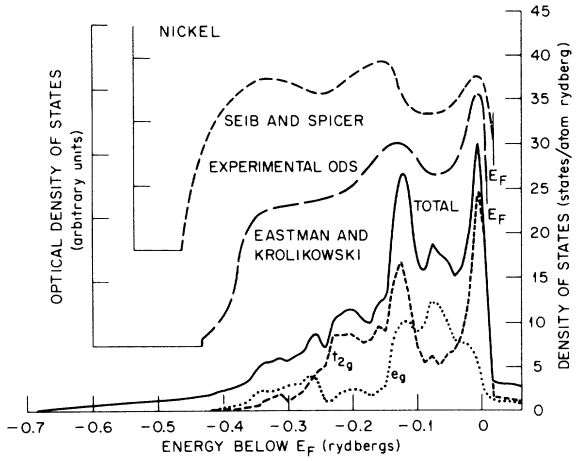

FIG. 1. Densities of states for pure paramagnetic Ni. Solid line: calculated total densities of states $\rho(E)$, short dashed line: t_{2g} component of the densities of states $\rho_T(E)$, dotted line: e_g component of the densities of states $\rho_E(E)$. The remaining lines are long dashed line: experimental ODS for Ni obtained by Eastman and Krolikowski, medium dashed line: experimental ODS for Ni obtained by Seib and Spicer. For the experimental curve the Fermi energy is as indicated; for the theoretical curves the zero of energy is the Fermi energy.

tive nature. Some of the salient work is contained in Refs. 31, 32, 42–45, 47–55, and references therein. A most thorough discussion of the basic features of the energy bands of Ni from an interpolative point of view is given by Zornberg[54] using a Mueller-type[56] interpolation scheme. For the present calculation we are interested in describing paramagnetic Ni, so much of Zornberg's analysis is not pertinent to the problem at hand. However, it is interesting to note that certain of the basic features of the bands obtained by Zornberg are in accord with the results of the present calculation. The interpolation procedure parameter set PS IV obtained by Zornberg and designated by him as one of his two best is shown in Table II transformed to a form compatible with the present notation (see Ref. 33). Note that in making the transformation we have used a value of $dd\pi$ which is the average of Zornberg's $dd\pi$ and $dd\pi'$. The parameters corresponding to the energy bands of Hanus, [50] the energy bands upon which the Cu-Ni alloy calculations of KVE were based, are also compared with the ones for the present potential in Table II. The most important of the parameters is E_0 since this fixes the position of the d-scattering resonance. The value obtained for E_0 using the present potential is in accord with the value found by Zornberg in his fit to experimental data, while the d bands of the Hanus potential are about 1 eV lower. The eigenvalues obtained for the present potential function at the L point are also in accordance with Zornberg's and others'[52] discussion of optical spectra in that $E(L_{32}) > E(L_{2'})$, the reverse being true of the Hanus calculation. The contrast between the positioning of the d bands and the level ordering at the L point for the present potential and that of Hanus is a direct reflection of the degree of d character of the atomic wave functions used to construct the two potentials, the Hanus potential being based on a $(3d)^8(4s)^2$ atomic configuration. Calculation reveals that for potentials constructed in the present manner that $L_{2'} > L_{32}$ for both $(3d)^8(4s)^2$ and $(3d)^9(4s)^1$ atomic configurations and that the corresponding values for E_0 are 0.481 and 0.519 Ry, respectively, the former being close to the value obtained for the Hanus potential.

At this stage it is worthwhile to consider the limitations which are imposed by the neglect of exchange splitting on comparisons between the densities of states functions obtained here for paramagnetic Ni and Cu-Ni alloys on the one hand and experimental data obtained on ferromagnetic Ni and Cu-Ni alloys on the other. Pierce and Spicer[57] have recently demonstrated that photoemission profiles from Ni are insensitive to the magnetic state of that metal and they place an upper bound on the exchange-splitting parameter of some 0.03 Ry at E_F. This value of the exchange-splitting parameter is in the general area found necessary by Zornberg and by other works. [33,48] From the present point of view the precise magnitude of the exchange splitting is not important, but the fact that it is small has important consequences. First, it makes comparisons between calculated densities of states and deep band probe experiments such as photoemission and soft-x-ray spectroscopy less questionable (subject to the considerations discussed in Sec. V). Second, the exchange splitting is small compared with the separation of 0.134 Ry between the d-scattering resonances of Cu and Ni that we use in the alloys. This then makes it appear that the effects of exchange splitting in ferromagnetic Cu-Ni alloys can be neglected within the present attempt to describe the gross effects of alloying on the densities of states, and that magnetic parts of the problem may be considered later as a perturbation.

In this connection it should be mentioned that Cooke and Davis[58] have used the potential function that we generated as a basis for some discussion of Stoner bands in Ni which have been measured by neutron diffraction. Their results indicate the same general positioning of the d bands and size of spin splitting discussed above.

Switendick has considered some ordered Cu-Ni alloys and has shown[59] that the density-of-states function obtained using the more standard methods

of band theory is similar in its general features to the ones we obtain with the CPA when a potential constructed as the present one is used.

For the above reasons we feel that the potential discussed at the first of this section yields a good description of the electronic states of paramagnetic Ni. In Secs. IV–VI, we will show that this same potential can be used to describe Cu-Ni alloys.

C. Copper

The Cu crystal potential was generated for an atomic configuration of $(3d)^{10}(4s)^{1}$. This potential function is essentially that of O'Sullivan, Switendick, and Schirber.[60] de Haas–van Alphen frequencies calculated using this potential function agree with the corresponding experimental quantities to an accuracy of > 1%. The lattice spacing used was 6.8032 a.u.

Eigenvalues for the set of $\vec{k}$ points over which the interpolation-Hamiltonian parameters were fitted are shown in Table I. The interpolation-Hamiltonian parameters which result from the fit are shown in Table II. Also shown in Table I are the corresponding parameters obtained by fitting the energy bands of Burdick.[61] In order to give the parameter sets a common base the Γ_1 eigenvalue was taken as the zero of energy. The fit to both sets of energy bands is generally better than 0.02 Ry being worse for points of low symmetry.

As may be seen from Table II, the parameters which result from the potential function generated here and the Chodorow[62] potential used by Burdick are quite similar. In particular, E_0 the parameter which positions the d-scattering resonance with respect to the sp band differs by only about 0.01 Ry between these two potential functions.

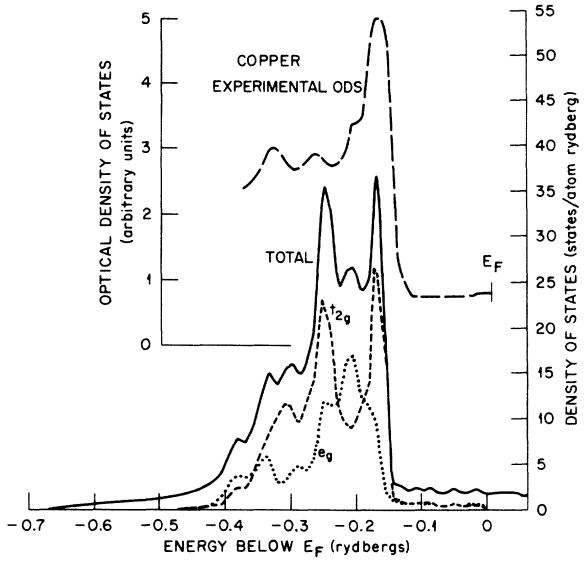

FIG. 2. Densities of states in pure Cu. The notation for the three lower curves is as in Fig. 1. Also shown are the experimental ODS results for Cu obtained by Krolikowski and Spicer. These have been drawn such that the high-energy peaks which occur in both theory and experiment coincide.

Figure 2 shows the total density of states (solid line) together with t_{2g} (short dashed line) and e_g (dotted line) components of the total densities of states for the present Cu potential. These are the Cu densities of states which are used in all subsequent calculations. Also displayed are the optical densities-of-states (ODS) results of Krolikowski and Spicer[63] obtained from analysis of photoemission data. Again the experimental curve has been drawn such that the high-energy peak in the ODS curve coincides with the position of the upper sharp peak in the calculated density-of-states curve; this procedure results in a mismatch of the Fermi energies of theory and experiment of some 0.01 Ry. The remaining structure in the ODS curve correlates well with structure in the density-of-states curve.

IV. RESULTS AND GENERAL DISCUSSION

CPA calculations of the density of states have been performed for a range of Cu-Ni alloys across the alloy diagram. The e_g and t_{2g} components of the density of states were obtained by solving Eqs. (9), (10), (13)–(15), and their equivalents for states of t_{2g} symmetry. The total densities of states were then obtained by adding the s densities of states. Partial densities of states were also calculated using equations such as (17). For all alloys the separation of the d-scattering resonances of Cu and Ni atoms is taken according to Eq. (7), or in the notation of Table II,

$$\delta = E_0^{\mathrm{Cu}} - E_0^{\mathrm{Ni}} \ . \tag{19}$$

Using the present potential functions $\delta = -0.134$ Ry, while the Hanus[50] Ni potential and the Burdick[62] Cu potential gives a value of 0.08 Ry, approximately that obtained by KVE. Calculations for Cu-rich alloys were based on the pure Cu densities of states shown in Fig. 2. Similarly, calculations for Ni-rich alloys were based on the pure-Ni densities of states shown in Fig. 1.

Figures 3–8 show the results of calculations of the total and partial densities of states, $\rho(E)$, $\rho^{\mathrm{Cu}}(E)$, and $\rho^{\mathrm{Ni}}(E)$ for the following alloy systems: 87% Cu, 13% Ni; 77% Cu, 23% Ni; 62% Cu, 38% Ni; 39% Cu, 61% Ni; 19% Cu, 81% Ni; and 11% Cu, 89% Ni—these alloy compositions corresponding to those used in the experimental work of Seib and Spicer.[14,25,26] In all of the figures $\rho(E)$ is given by the full line, $\rho^{\mathrm{Cu}}(E)$ by the medium dash, $\rho^{\mathrm{Ni}}(E)$ by the short dash. The zero of energy is the Fermi energy drawn for an electron-to-atom ratio ap-

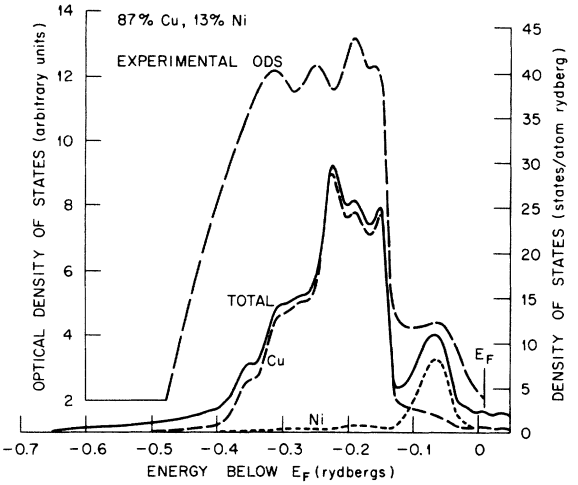

FIG. 3. Densities of states for a 87% Cu, 13% Ni alloy calculated using the CPA. Solid line: total densities of states $\rho(E)$, medium dashed line: contribution to the densities of states from Cu sites $\rho^{Cu}(E)$, short dashed line: contribution to the deisities of states from Ni sites. Also shown are the experimental ODS of Seib and Spicer. The experimental ODS have been moved such that the edge at ≈ -0.16 Ry coincides with the theoretical curve. Fermi energy is marked as E_F. For the theoretical curves the zero of energy is the Fermi energy.

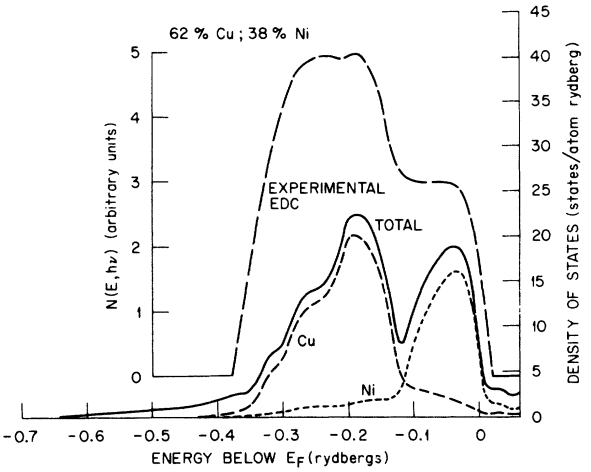

FIG. 5. Densities of states for a 62% Cu, 38% Ni alloy using the CPA . For the lower theoretical curves the notation is as in Fig. 3. Also shown is a experimental electron-distribution curve taken from the photoemission work of Seib and Spicer. The EDC is for an incident photon energy of 10.2 eV.

propriate to the alloy in question, i.e.,

$$\mathfrak{z}^{\text{alloy}} = 10 + c \ , \tag{20}$$

where c is the Cu concentration.

From Figs. 1–8 a clear picture of the behavior of the densities of states as a function of concentration is presented from the case of pure Cu through pure Ni. The picture is that on the addition of small amounts of Ni to Cu an impurity d subband associated with Ni sites forms between the d-band structure associated with the Cu sites and the Fermi energy. The reduction of order upon the addition of Ni results in some loss of structure in the Cu d bands particularly at the top of the band. For small concentrations of Ni the impurity subband is Lorentzian in shape. On the addition of more Ni the impurity subband grows at the expense of the host subband which continues to lose structure, until for concentrations of Ni in the region of 25% the sharp high-energy (-0.16 Ry) peak which is present in pure Cu is completely damped out. For Ni concentrations in excess of 40%, the Ni d subband starts to develop small amounts of structure; on the addition of greater amounts of Ni

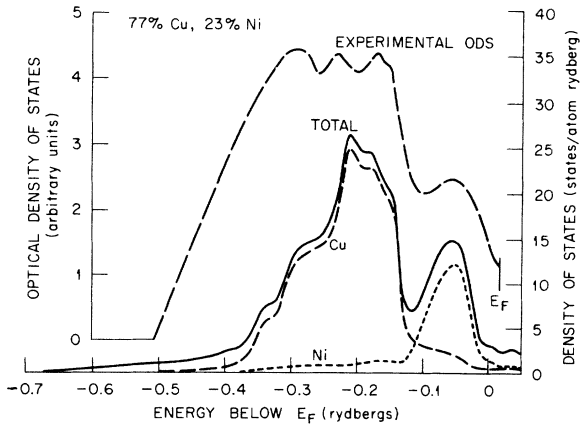

FIG. 4. Densities of states for a 77% Cu, 23% Ni alloy calculated using the CPA. The notation is as in Fig. 3.

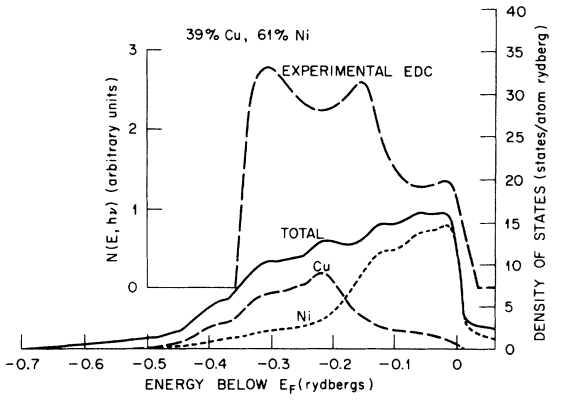

FIG. 6. Densities of states for a 39% Cu, 61% Ni alloy calculated using the CPA. The notation is as in Fig. 5. The EDC is for an incident photon energy of 10.0 eV and was taken from the work of Seib and Spicer.

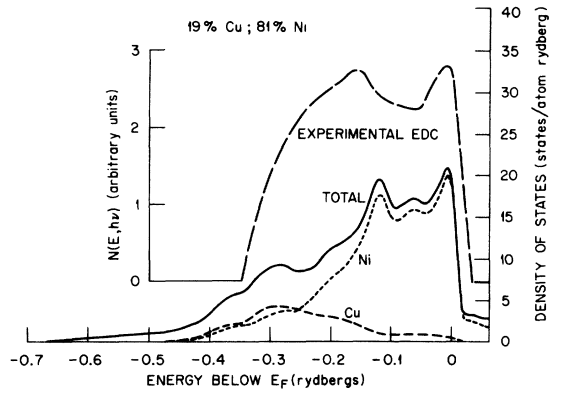

FIG. 7. Densities of states for a 19% Cu, 81% Ni alloy calculated using the CPA. The notation is as in Fig. 5. The EDC is for an incident photon energy of 10.0 eV and was taken from the work of Seib and Spicer.

the Ni subband continues to grow at the expense of the Cu subband finally evolving into the Ni d-band structure in which the Fermi energy lies. During this whole process the host and impurity subbands change their general position with respect to the Fermi energy very little.

Total d charges associated with Cu and with Ni sites were obtained from values of E_F calculated from the total densities of states and from the partial densities-of-states functions ρ^{Cu} and ρ^{Ni}. These show that the charge on these sites remains as that for the pure metals, which is consistent with the minimum polarity model of Lang and Ehrenreich.[64] This also substantiates the choice of the pure-metal neutral-atom configuration model for the alloy upon which the calculations are based.

Before giving detailed discussion of the present results in the light of available experimental information it is useful to consider the role of the magnitude of the splitting between the d-scattering resonances of the two atomic species in the alloy. This has already been studied in the context of a simplified densities-of-states function[9] but is worthy of further stressing here. Figure 9 shows the effect of setting δ at a series of hypothetical values for a 87% Cu, 13% Ni alloy. In this figure are plotted the total densities of states for a range of values of δ from 0 to 0.134 Ry. Again in Fig. 9 the zero energy is the Fermi energy for a z corresponding to a 87% Cu, 13% Ni alloy, where z is the electron-to-atom ratio.

The uppermost ($\delta = 0.0$ Ry) curve of Fig. 9 corresponds simply to the predictions of the rigid-band model for this system. The effect in the CPA of increasing δ in the direction of its calculated value in Cu-Ni alloys can be seen clearly in the gradual detachment of the impurity d subband from the main host subband, the degree being simply related to the magnitude of δ. The value of δ obtained by KVE in their work on Ni-rich Cu-Ni alloys would result in no detachment of the Ni subband for Cu-rich Cu-Ni alloys (see $\delta = -0.060$ Ry curve), but simply the formation of a shoulder.

Increasing the magnitude of δ has another interesting consequence. As δ is increased the separation between the high-energy peak in the main d band and the Fermi energy is increased. For $\delta = -0.134$ Ry this increase almost completely compensates for the decrease in z which results from the addition of Ni impurities.

In a very Ni-rich Cu-Ni alloy (say 10% Cu) consideration of the role of δ shows that the gross structure in the total density of states is changed little on increasing δ from 0 Ry (see pure Ni curve of Fig. 1) to 0.06 Ry (see 10% Cu, 90% Ni curve of KVE) to 0.134 Ry (see Fig. 8 of this work). This relative independence of the gross structure of $\rho(E)$ for extremely Ni-rich alloys (< 20% Cu) on the magnitude of δ has already been noted by KVE.

This extreme asymmetry in the behavior of the densities of states for Cu-Ni alloys can easily be understood in terms of the steeple model of KVE in that at the high-energy edges the d bands of Cu and Ni are extremely sharp and peaked while the density of states at the low-energy edge is rather low. Use of the Slater-Koster[9,65] criterion for the formation of an impurity level and reasonable band edges for the t_{2g} and e_g densities of states for Cu and Ni show that the value of δ required to split off an impurity level from the bottom of the Ni d band (δ_{SK}^{Ni}) and the corresponding value to split off an impurity level from the top of the Cu d band (δ_{SK}^{Cu}) are -0.42 and -0.07 Ry, respectively. From this it can be seen that the actual magnitude of δ for Cu-Ni alloys is of the same order as δ_{SK}^{Cu} but is very much smaller than δ_{SK}^{Ni}. Thus the densities

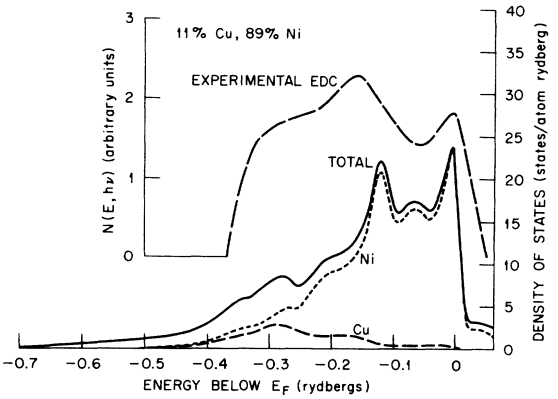

FIG. 8. Densities of states for a 11% Cu, 89% Ni alloy calculated using the CPA. The notation is as in Fig. 5. The EDC is for an incident photon energy of 10.0 eV and was taken from the work of Seib and Spicer.

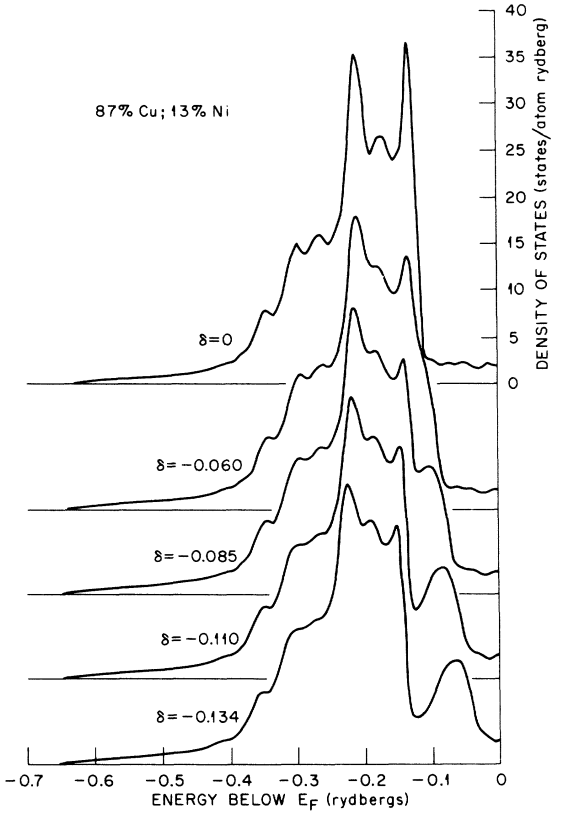

FIG. 9. Effect of increasing the separation in energy between the d-scattering resonances associated with Cu and Ni sites in a random 87% Cu, 13% Ni alloy calculated using the CPA. $\delta = 0$ Ry corresponds to the rigid-band model, $\delta = -0.060$ Ry corresponds to using the value of δ obtained by KVE, $\delta = -0.134$ Ry corresponds to the present calculations.

of states of Cu-rich Cu-Ni alloys are very sensitive to the precise magnitude of δ while those of Ni-rich Cu-Ni alloys are not.

V. COMPARISON WITH EXPERIMENT

A. Photoemission Spectra

Conventional interpretations of the photoemission spectra from pure Cu[26,63] and pure Ni[46] have been in terms of the underlying densities of states in these metals. It is therefore useful to see if the recent photoemission spectra obtained by Seib and Spicer for a series of Cu-Ni alloys can also be understood in terms of the densities-of-states functions calculated here.

Photoemission is usually regarded as a three-stage process: optical excitation of the electrons in the bulk of the sample, transport of the excited electrons to the surface of the material, and escape of the electrons from the surface.

Within the framework of a model in which it is assumed that the optical transitions are nondirect (i.e., the reduced $\vec{k}$ vectors of the initial and final states of the excited electron are not constrained to be equal) and of $\vec{k}$ and energy-independent optical matrix elements, the photoemission profile is simply related to a folded optical density of states $\rho_{\mathrm{FODS}}(E, h\nu)$ which is the product of the densities of initial (filled) and final (empty) densities of states[66]

$$\rho_{\mathrm{FODS}}(E, h\nu) = \rho_i(E - h\nu)\rho_f(E) , \tag{21}$$

where $h\nu$ is the incident photon energy. By using photoemission profiles for a number of incident photon energies it is possible after making assumptions about the processes involved in the transport of the photoemitted electrons to the surface of the material and their subsequent emission from the surface to obtain an unfolded experimental ODS function. The ODS of Seib and Spicer[25] and Eastman and Krolikowski[46] for Ni and of Krolikowski and Spicer[63] for Cu displayed in Figs. 1 and 2 were obtained using the nondirect transition model. Leaving aside questions concerning the applicability of this model in detail, it is clear that structure in the ODS is in a one-to-one correspondence with the major structure in the calculated density-of-states function.

The experimental ODS of Seib and Spicer for 87% Cu, 13% Ni and 77% Cu, 23% Ni alloys are shown as the long dashed curves on Figs. 3 and 4, respectively. Again structure in the ODS reflects quite well certain features of the theoretical density of states for both these alloys. This is particularly true of the leading edge of the Cu d bands and the structure some 0.07 Ry below E_F, which is not present in the ODS of pure Cu. This latter structure is seen to be associated with that in the calculated density-of-states function which results from the formation of the Ni impurity d subband. The relative magnitudes of the calculated host and impurity subbands appears also to be reflected in the ODS. Seib and Spicer explained the appearance of the impurity subband in terms of a Friedel-Anderson virtual-bound-state model. As noted in Ref. 10, the results presented above are quite consistent with the virtual-bound-state model. For small Ni impurity concentrations the impurity d subband is Lorentzian in shape as would be expected from the virtual-bound-state model. The calculated position of the Ni subband being 0.68 and 0.79 Ry above the high-energy edge of the Cu subband for the 13% Ni and 23% Ni alloys, respectively, the calculated half-width of the impurity subbands being 0.034 and 0.042 Ry. The corresponding experimental values are 0.74 and 0.81 Ry for the position of the center of the impurity subband with respect to the host subband and 0.040 and 0.048 Ry for the half-widths. It should be emphasized at this point that although the virtual-bound-state model gives

qualitatively the same picture as the CPA for these dilute Ni alloys these CPA calculations represent the first semiquantitative description of the densities of states in these Cu-rich alloys. Also, unlike the virtual-bound-state model, the CPA is not restricted to the low-Ni-concentration regime.

The calculated behavior of the Cu d subband on the addition of Ni to Cu is also in general agreement with that observed in the ODS, the important features of the Cu subband being the almost complete independence of the location of its high-energy edge on Ni concentration coupled with the rapid loss in magnitude of the high-energy (~ -0.16 Ry) peak in the Cu subband as Ni is added (Figs. 2–4). This peak which is sharp and pronounced in pure Cu is reduced considerably in the 13% Ni alloy and is damped to a shoulder in the 23% Ni alloy; this is consistent with the experimental ODS curves. This behavior of the high-energy edge from the Cu d band has been more fully described in an earlier paper[10] where it was shown that this behavior together with the formation of a Ni impurity subband cannot be explained using either the rigid-band model or the virtual-crystal approximation.

For alloys having Ni concentrations of greater than 23% it is more difficult to compare the densities-of-states functions calculated here with the corresponding photoemission data of Seib and Spicer[26,27] since ODS have not been given. However sufficient information about peak positions can be obtained from the electron distribution curves (EDC's) of Seib and Spicer to suggest that the present calculated densities-of-states functions are quite consistent with this experimental data.

From Eq. (21) it is clear that if there is little structure in the unfilled region of the densities of states and the EDC's are referred to an initial-state energy $E - h\nu$ (or more usually $E + \phi - h\nu$, where ϕ is the sample work function), then structure in the EDC's will superpose and will directly reflect structure in the filled region of the density-of-states function. This superposition of structure in the EDC's when referred to initial-state energy is a well-known situation for many metals and is the observed behavior in the photoemission spectra of Seib and Spicer for alloys of Cu and Ni of all concentrations. EDC's typical of each alloy system having Ni concentrations of 38, 61, 81, and 89% are shown as the outer long dashed curves of Figs. 5–8, respectively. The EDC for the 38% alloy is for an incident photon energy of 10.2 eV. The rest are for an incident photon energy of 10.0 eV.

Figure 5 shows the effect of increasing the Ni concentration above that of Figs. 3 and 4. Structure has been almost totally removed from the Cu subband and the Ni impurity subband has grown to a size comparable with that of the Cu subband. This appears to be reflected in the two broad structureless peaks observed in the photoemission (that the two peaks are not resolved in any single EDC is probably due to internal scattering process which the photoemitted electron undergoes during its transport to the surface of the sample). By using EDC's for a series of incident photon energies (see Figs. VI. 1 and VI. 2 of Ref. 27) the general features of the present densities-of-states function for this alloy can be further substantiated and the picture of a Cu subband and Ni subband in approximately the same positions with respect to E_F as in the 13 and 23% Ni alloys emerges.

Of all the alloys considered here structure in the EDC's for the 39% Cu, 61% Ni alloy (Fig. 6) correlates least well with structure in the calculated densities of states. The reasons for this probably partly lie in the uncertainties in the calculation, these being greatest for near equiatomic alloys. Also it is well known that clustering of Ni atoms is likely to occur in Cu-Ni alloys in this concentration range (see Ref. 16 for a thorough discussion and for other pertinent references). That clustering is in some part a cause of the greater structure observed in the EDC's than one would expect from the calculated density-of-states curve is indicated in the positions of the two high-energy peaks, these peaks falling in positions typical of more Ni-rich Cu-Ni alloys or indeed pure Ni. As is clear from the position of the Ni subband in this alloy and alloys more rich in Ni (see Figs. 7 and 8) structure from Ni-rich regions of the alloy would superpose on the small amount of structure which is already present in the calculated densities of states for the perfectly random alloy which the calculation represents.

Structure in the EDC's for the 19% Cu, 81% Ni and 11% Cu, 89% Ni alloys (Figs. 7 and 8) again correlates well with the structure in the calculated density-of-states function. The correlation being at least as good as the corresponding correlation for pure Ni. As with pure Ni only two peaks are resolved in the photoemission spectra; as with pure Ni the separation between the two peaks in the EDC's is somewhat greater than the separation between the two main peaks in the density-of-states function. However comparison of the ODS obtained by Seib and Spicer with those obtained by Eastman and Krolikowski for pure Ni shows that the disparity between these two experiments in respect of the separation between the two main peaks is as great as the disparity between the theoretical densities of states and the experiment in this one respect.

Although from the point of view of the foregoing discussion it is clear that the present densities-of-states functions calculated for Cu-Ni alloys are consistent with the experimental photoemission

results of Seib and Spicer, the discussion must be treated with some caution because of a lack of a sound theoretical understanding of the photoemission process. The respective roles of direct ($\vec{k}$-conserving) and nondirect optical transitions in the spectra of pure metals are not well understood, it being possible to interpret the photoemission spectra from pure Cu entirely in terms of a direct transition model[67] as well as the nondirect transition model assumed here. Also Schaich and Ashcroft[68] have pointed to the effects of the surface in distorting photoemission spectra, effects which they indicate may be of the same order as those resulting from bulk states for pure Cu and pure Ni. From the present point of view we would only comment that for alloys the role of $\vec{k}$ conservation would be expected to be decreasingly important as the disorder in the system increases. Also we are interested only in establishing a correlation between the *chief* features of the present calculations with the *gross* structure of the photoemission data of Seib and Spicer.

At this point it is also worthwhile to comment on the optical reflectivity spectra obtained by Seib and Spicer[14,26,27] for Cu-Ni alloys. Of this data perhaps the most outstanding feature is the pronounced changes which the reflectivity undergoes for photon energies in the range of 0–2 eV when small amounts of Ni are added to pure Cu. These changes are interpreted by Seib and Spicer in terms of the virtual-bound-state model, since for these alloys the predictions of the CPA and the qualitative features of the virtual-bound-state model are essentially the same; the reflectivity results are also qualitatively consistent with the present calculations. For alloys very rich in Ni the reflectivity data is relatively independent of the Ni concentration. This is again consistent with the present calculations in that structure in the densities of states of very Ni-rich Cu-Ni alloys is relatively independent of Ni concentration and is very similar to structure present in pure Ni.

B. Soft-X-Ray Spectra

The emission of a soft-x-ray photon from a metal or alloy results from the filling of some previously created hole in a core level of an atom in the bulk of the material by an electron from the conduction band, the hole in the atom usually being in the $1s$ (K emission), $2p$ ($L_{II,III}$ emission), or $3p$ ($M_{II,III}$ emission) shells.

There have been a number of studies of Cu-Ni alloys using the soft-x-ray emission experiment; chief among these are Farineau and Morand[27] (L spectra); Friedman and Beeman[28] (K spectra); and Clift, Curry, and Thompson[29] (M spectra). Azároff and Das[69] have studied the soft-x-ray K absorption spectra of Cu-Ni alloys. There have also been a number of studies made of pure Cu and pure Ni; see, for example, Dobbyn *et al.*[70] (Cu) and Cuthill *et al.*[71] (Ni).

From the viewpoint of studying the electronic states in alloys the soft-x-ray emission is potentially a very powerful tool since the information which is obtained from the experiment is presumably local in character, giving information about electrons in the neighborhood of the emitting atom. For a binary alloy two emission profiles are observed, one corresponding to each atomic species in the alloy. This is a trivial consequence of the separation between a particular level of one atomic species and that of the other atomic species. For the K, $L_{II,III}$, and $M_{II,III}$ emission profiles of Cu-Ni alloys this natural separation is sufficiently great to resolve the individual profiles although there is overlap between the $M_{II,III}$ complexes for Ni and for Cu sites.

Calculation of the soft-x-ray profiles for an arbitrary alloy is a formidable task since knowledge is required of the imaginary part of the restricted averaged Green's function[72] $\langle G(r, r'; E)\rangle_{R,\xi}$ where the subscripts denote that the average is restricted to require occupancy of the site R by the atomic species ξ. Within the present model we have obtained the partial d densities of states $\rho^{Cu}(E)$ and $\rho^{Ni}(E)$ which are related to the restricted average Green's function through equations such as (16). While it is not meaningful to compare details in the structure in the site-dependent densities-of-states functions with the corresponding emission profiles it is clear that the general position in energy of the emission profiles and the position of the absorption edges in the soft-x-ray data should reflect the position of the high density-of-states regions of $\rho^{Cu}(E)$ and $\rho^{Ni}(E)$ and the position of E_F.

The important feature of the experimental Cu and Ni soft-x-ray profiles and absorption edges in Cu-Ni alloys is their independence of the composition of the alloy. The position and shape of the Cu and Ni $M_{II,III}$ emission profiles are completely independent of the concentrations of Ni and Cu in the alloy. The over-all positions of the Cu and Ni $L_{II,III}$ profiles are also independent of concentration, although the Ni $L_{II,III}$ profile does narrow somewhat as the Ni concentration is decreased and the Cu $L_{II,III}$ profile shows some change in structure for very small concentrations of Cu. The positions of the Cu and Ni K emission profiles are again quite independent of alloy concentration although structure within these profiles does depend on alloy composition, becoming more smeared as the concentration of the emitting atom is decreased. The positions of the Cu and Ni K absorption edges are independent of the alloy concentration to an accuracy of some 0.3 eV.

The behavior detailed above is largely consistent

with the densities of states presented here. The Fermi energy, and hence the K absorption edge, is independent of concentration to accuracy of some 0.4 eV; this feature of the results has already been discussed above in respect of the photoemission profiles. The independence of alloy composition of the position of the Cu and Ni $L_{II,III}$ and $M_{II,III}$ and K emission profiles is also completely consistent with the calculated $\rho^{Cu}(E)$ and $\rho^{Ni}(E)$, the high density-of-states region of the calculated $\rho^{Cu}(E)$ and $\rho^{Ni}(E)$ being centered around the same energy ($\frac{1}{2}\delta$ and $-\frac{1}{2}\delta$) for all the alloys. More precisely a contribution to these partial densities of states from the sp band should be added in, but within the present framework this can be neglected since it is rather structureless compared with the contribution from the d bands. Changes in structure within the high density-of-states part of $\rho^{Cu}(E)$ and $\rho^{Ni}(E)$ are clearly not reflected by the $M_{II,III}$ soft-x-ray emission profiles, but this is perhaps not surprising since calculations[70] have revealed that structure present in the densities-of-states functions for pure metals is generally smoothed when the full variation of the transition matrix elements are properly accounted for. The observed narrowing of the Ni $L_{II,III}$ profile may be related to the narrowing of the Ni d subband as the Ni concentration becomes small. However, if this is the case, it is then not clear why a similar narrowing is not observed in the $M_{II,III}$ profile. Within the framework of the present cursory look at the soft-x-ray profiles of Cu-Ni alloy it is not possible to account for the apparent concentration dependence of the shape of the Cu and Ni K emission and absorption profiles from Cu-Ni alloys.

Full calculations of the Cu and Ni soft-x-ray emission profiles within the CPA framework are obviously required before the above discussion can be carried further, but it does appear that the Cu-Ni alloy system does represent a particularly simple system where such calculation could be expected to result in some success.

C. Low-Temperature Specific Heat

In the simplest of theories of low-temperature specific heat, the coefficient (γ) of the term linear in temperature is related to the electronic density of states at the Fermi energy $\rho(E_F)$ through

$$\gamma = \tfrac{1}{3}\pi^2 k_B^2 \rho(E_F) \quad . \tag{22}$$

The banded region of Fig. 10 shows the results of calculating γ for Cu-Ni alloys using the above CPA results. The upper bound is the result of basing the calculations across the complete concentration range on the densities of states for pure Cu. The lower bound results from similar calculations based on pure Ni. For $c < 50\%$, the lower bound would be the more reasonable values to use; for $c > 50\%$, the upper bound would represent the more reasonable values. The monotonic rise in γ as a function of concentration for Ni impurities of greater than 35% is simply a consequence of the fact that at approximately this concentration the Ni subband (which is present for all finite concentrations of Ni) has grown so that the high density-of-states part of it intersects with E_F. As the concentration of Ni is further increased the size of the Ni subband increases and consequently the magnitude of $\rho(E_F)$ rises also. For Ni concentrations of $< 30\%$ the main part of the Ni impurity subband is not sufficiently large to intersect the Fermi energy. Therefore $\rho(E_F)$ is typical of an s band being small and relatively independent of concentration.

Experimentally determined values of γ are also shown in Fig. 10, these being the data of Dixon *et al.*[73] There is a great deal of additional data which have not been included (for example, Gupta *et al.*[74] and Robbins *et al.*[75]) since these data are in general accord with that displayed. For very Cu-rich alloys the agreement between the theoretical and experimental curves is good. However for more Ni-rich alloys differences in the shapes of the theoretical and experimental curves become pronounced. These discrepancies in shape are real and point to the large effects which are known to arise from magnetic interactions, electron-phonon interaction, and clustering in these alloys. The general shape of the theoretical curve of γ as a function of concentration of Fig. 10 is in good accord with the corresponding experimental plot for Ag-Pd alloys,[76] this system being in many respects like Cu-Ni except that it is not ferromagnetic. This tends to support the conclusion that Fig. 10 represents a good estimate of the best which can be obtained from a simple paramagnetic theory of these alloys.

It is worth commenting on the similarities of the predictions of the CPA, the rigid-band model, and the virtual-crystal approximation in respect of the general shape of plots of $\rho(E_F)$ (and hence γ) against c (see, for example, Fig. 3 of Lee and Lewis[77]). This similarity is purely coincidental since for a given alloy the densities of states obtained using the CPA in no way resemble those from the other calculations (see Fig. 9). Thus the simple fact that the shape of a plot of γ against c obtained from a model is in agreement with experiment does not establish the correctness of the model for the alloy in question.

Before closing this section it should be noted that the onset of ferromagnetism in Cu-Ni alloys occurs for a Ni concentration of approximately 44%.[78,79] Clearly from Fig. 10 and the earlier figures this composition corresponds to a region where the Fermi energy lies in the d bands of the alloy. The d states near the Fermi energy are primarily at

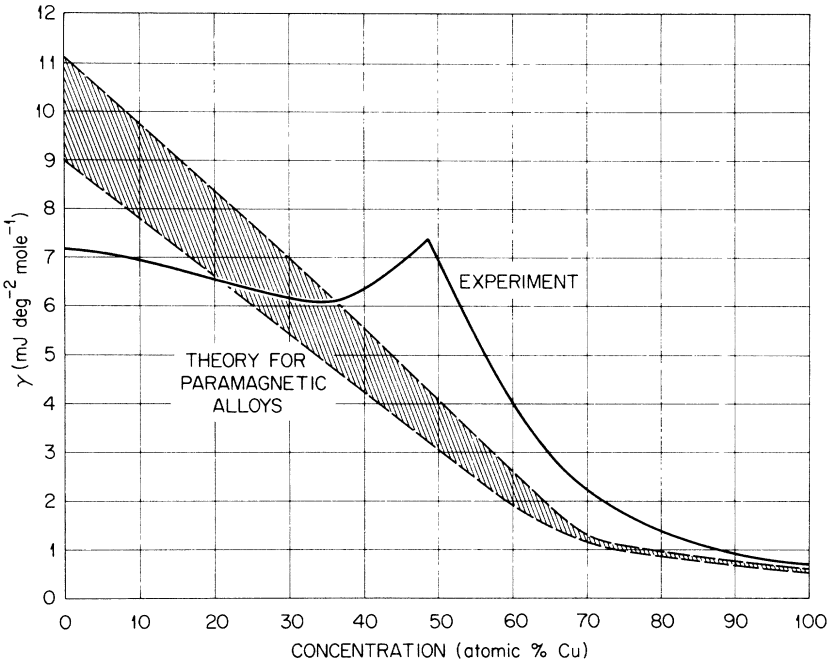

FIG. 10. Low-temperature specific-heat coefficient γ plotted as a function of Cu concentration for Cu-Ni alloys. The shaded area indicates the results of the present CPA calculations for paramagnetic Cu-Ni alloys. For $c < 50\%$ the lower bound would be the more appropriate. The experimental curve is taken from Dixon *et al.* (Ref. 73).

Ni sites and largely of t_{2g} symmetry; as mentioned earlier this is consistent with the minimum polarity description of Cu-Ni alloys used by Lang and Ehrenreich in their discussion of ferromagnetism in Cu-Ni alloys.

VI. SUMMARY

The densities of states of Cu-Ni alloys appear to be well described by the coherent-potential approximation; in particular if care is taken in choosing the potential functions to be associated with Cu and with Ni sites in the alloy then the simple model proposed by Kirkpatrick, Velický, and Ehrenreich for describing Ni-rich alloys of Cu-Ni can be readily extended to describing Cu-Ni alloys of arbitrary concentration. The results presented above are consistent with experimental photoemission and soft-x-ray spectroscopy data in so far as comparisons with data of this type can be effected without detailed and perhaps unreliable calculations of the emission profiles. The results also point to the large effects of the electron-phonon interaction, magnetic interactions, and clustering of Ni atoms which occur in this alloy system and are manifest in measurements of the low-temperature specific-heat coefficient γ.

The calculations were based on models of pure metallic Cu and Ni which are based on potential functions generated from a simple muffin-tin superposition of atomic potentials and full Slater exchange, the basic atomic configurations used for Cu and Ni being $(3d)^{10}(4s)^{1}$ and $(3d)^{9.4}(4s)^{0.6}$, respectively. Calculations of partial densities of states associated with Cu and with Ni sites as well as total charges of d character for Cu and Ni sites reveals that the sites retain much of the identity which they possessed in the pure metal. In alloys of Cu-Ni, Cu d states are located in the energy region associated with Cu d states in metallic Cu and similarly Ni d states are located in the energy region associated with Ni d states in metallic Ni. For Cu-rich Cu-Ni alloys this results in the formation of separate Cu and Ni bands, bands which are observed in photoemission experiments as well as soft-x-ray spectroscopy measurements. In Ni-rich Cu-Ni alloys the Cu and Ni d bands overlap and are only individually distinguishable in the soft-x-ray emission experiment. For very Ni-rich alloys the present results are essentially those of Kirkpatrick *et al.*

For all alloys the previously used rigid-band model and virtual-crystal approximation are totally inadequate for describing the d states in these alloys. This is particularly manifest for alloys rich in Cu where a clear split-band regime pertains, since neither of these models are capable even in principle of describing such a two-band regime. For alloys very rich in Cu the results of these coherent-potential-approximation calculations are in agreement with the qualitative features of the virtual-bound-state model of Anderson and Friedel.

ACKNOWLEDGMENTS

We would like to thank Dr. H. Ehrenreich and

Dr. W. E. Spicer for helpful communications. We would also like to thank Dr. L. Hodges for sending us a copy of his interpolation program against which our program could be checked.

---

*Research sponsored by the U. S. Atomic Energy Commission under contract with the Union Carbide Corp.

†Present address: University of Vermont, Burlington, Vt. 05401.

[1]P. Soven, Phys. Rev. 156, 809 (1967); 178, 1136 (1969).

[2]See, for example, J. Friedel, Nuovo Cimento Suppl. 7, 287 (1958).

[3]L. Nordheim, Ann. Physik 9, 607 (1931); 9, 641 (1931).

[4]T. Muto, Sci. Papers Inst. Phys. Chem. Res. (Tokyo) 34, 377 (1938).

[5]J. Friedel, Can. J. Phys. 34, 1190 (1956); J. Phys. Radium 19, 573 (1958).

[6]P. W. Anderson, Phys. Rev. 124, 41 (1961).

[7]B. Velický, S. Kirkpatrick, and H. Ehrenreich, Phys. Rev. 175, 747 (1968).

[8]For a review see J. S. Faulkner, Intern. J. Quantum Chem. (to be published).

[9]S. Kirkpatrick, B. Velický, and H. Ehrenreich, Phys. Rev. B 1, 3250 (1970).

[10]G. M. Stocks, R. W. Williams, and J. S. Faulkner, Phys. Rev. Letters 26, 253 (1971).

[11]K. Levin and H. Ehrenreich, Phys. Rev. B 3, 4172 (1971).

[12]G. M. Stocks, Intern. J. Quantum Chem. (to be published).

[13]D. Stroud and H. Ehrenreich, Phys. Rev. B 2, 3197 (1970).

[14]D. H. Seib and W. E. Spicer, Phys. Rev. B 2, 1676 (1970).

[15]A. P. Klein and A. J. Heeger, Phys. Rev. 144, 458 (1966).

[16]C. L. Foiles, Phys. Rev. 169, 471 (1968).

[17]J. Korringa, J. Phys. Chem. Solids 7, 252 (1958).

[18]J. L. Beeby, Phys. Rev. 135, A130 (1964); Proc. Roy. Soc. (London) A279, 82 (1964).

[19]J. S. Faulkner and J. Korringa, Phys. Rev. 122, 390 (1961).

[20]P. Soven, Phys. Rev. 151, 539 (1966).

[21]P. W. Anderson and W. L. McMillan, in *Proceedings of the International School of Physics "Enrico Fermi," Course* 37, edited by W. Marshall (Academic, New York, 1967).

[22]J. M. Ziman, Advan. Phys. 13, 89 (1964).

[23]A. Meyer, C. W. Nestor, Jr., and W. H. Young, Proc. Phys. Soc. (London) 92, 446 (1967).

[24]G. M. Stocks and W. H. Young, J. Phys. C 2, 680 (1969).

[25]D. H. Seib and W. E. Spicer, Phys. Rev. B 2, 1694 (1970).

[26]D. H. Seib, Stanford Electronics Laboratories Technical Report No. 5227-1 (unpublished).

[27]J. Farineau and M. Morand, J. Phys. Radium 10, 447 (1938).

[28]H. Friedman and W. W. Beeman, Phys. Rev. 58, 400 (1940).

[29]J. Clift, C. Curry, and B. J. Thompson, Phil. Mag. 8, 593 (1963).

[30]J. C. Love, F. E. Obenshain, and G. Czjzek, Phys. Rev. B 3, 2827 (1971).

[31]L. Hodges, thesis (Harvard University, 1966) (unpublished).

[32]L. Hodges, H. Ehrenreich, and N. D. Lang, Phys. Rev. 152, 505 (1966).

[33]L. Hodges and H. Ehrenreich, in *Methods in Computation Physics*, edited by B. Alder, S. Fernbach, and M. Rotenberg (Academic, New York, 1968).

[34]J. Korringa, Physica 13, 392 (1947).

[35]W. Kohn and N. Rostocker, Phys. Rev. 94, 1111 (1954).

[36]L. F. Mattheiss, Phys. Rev. 133, 184 (1964).

[37]F. Herman and S. Skillman, *Atomic Structure Calculations* (Prentice-Hall, Englewood Cliffs, N. J., 1963). The charge densities used were obtained directly from a modified version of the Herman-Skillman program.

[38]R. Latter, Phys. Rev. 99, 510 (1955); see Ref. 37, Sec. 1.

[39]J. C. Slater, Phys. Rev. 81, 385 (1951).

[40]J. S. Faulkner, Bull. Am. Phys. Soc. 16, 313 (1971).

[41]J. S. Faulkner, H. L. Davis, and H. W. Joy, Phys. Rev. 161, 656 (1967).

[42]J. W. D. Connolly, Phys. Rev. 159, 415 (1967).

[43]J. Yamashita, M. Fuckuchi, and S. Wakoh, J. Phys. Soc. Japan 18, 999 (1963).

[44]E. C. Snow, J. T. Waber, and A. C. Switendick, J. App. Phys. 37, 1342 (1966).

[45]E. C. Snow and J. T. Waber, Acta Met. 17, 623 (1969).

[46]D. E. Eastman and W. F. Krolikowski, Phys. Rev. Letters 21, 623 (1968).

[47]H. Ehrenreich, H. R. Philipp, and D. J. Olechna, Phys. Rev. 131, 2469 (1963).

[48]J. C. Phillips, Phys. Rev. 133, A1020 (1964).

[49]L. F. Mattheiss, Phys. Rev. 134, 192 (1964).

[50]J. G. Hanus, Massuchusetts Institute of Technology, Solid State and Molecular Theory Group Quarterly Progress Report No. 44, 1961 (unpublished).

[51]S. Wakoh and J. Yamashita, J. Phys. Soc. Japan 19, 1342 (1964).

[52]J. Hanus, J. Feinleib, and W. J. Scouler, Phys. Rev. Letters 19, 16 (1967).

[53]J. Ruvolds and L. M. Falicov, Phys. Rev. 172, 508 (1968).

[54]E. I. Zornberg, Phys. Rev. B 1, 244 (1970).

[55]J. Calloway and H. M. Zhang, Phys. Rev. B 1, 305 (1970).

[56]F. M. Mueller, Phys. Rev. 153, 659 (1967).

[57]D. T. Pierce and W. E. Spicer, Phys. Rev. Letters 25, 581 (1970).

[58]J. F. Cooke and H. L. Davis, Bull. Am. Phys. Soc. 16, 350 (1971).

[59]A. C. Switendick, Bull. Am. Phys. Soc. 16, 404 (1971).

[60]W. J. O'Sullivan, A. C. Switendick, and J. E. Schirber, Phys. Rev. B 1, 1443 (1970).

[61]G. A. Burdick, Phys. Rev. 129, 138 (1963).

[62]M. Chodorow, Phys. Rev. 55, 675 (1939); Ph. D. thesis (Massachusetts Institute of Technology, 1938) (unpublished).

[63]W. Krolikowski and W. E. Spicer, Phys. Rev. 185, 882 (1969).

[64]N. D. Lang and H. Ehrenreich, Phys. Rev. 168, 605 (1968).

[65]G. F. Koster and J. C. Slater, Phys. Rev. 96, 1208 (1954).

[66]C. N. Berglund and W. E. Spicer, Phys. Rev. 136, A1030 (1964).

[67]N. V. Smith, Phys. Rev. B 3, 1862 (1971).

[68]W. L. Schaich and N. W. Ashcroft, Solid State Commun. 8, 1959 (1970); Phys. Rev. B 3, 2452 (1971).

[69]L. V. Azároff and B. N. Das, Phys. Rev. 134, A747 (1964).

[70]R. C. Dobbyn, M. L. Williams, J. R. Cuthill, and A. J. McAlister, Phys. Rev. B 2, 1563 (1970).

[71]J. R. Cuthill, A. J. McAlister, M. L. Williams, and R. C. Dobbyn, *Soft X-Ray Band Spectra*, edited by D. J. Fabian (Academic, New York, 1968).

[72]B. L. Gyorffy and M. J. Stott, Solid State Commun. 9, 613 (1971).

[73]M. Dixon, F. E. Hoare, and T. M. Holden, Proc. Roy. Soc. (London) A303, 339 (1968).

[74]K. P. Gupta, C. H. Cheng, and P. A. Beck, Phys. Rev. 133, A203 (1964).

[75]C. G. Robbins, H. Claus, and P. A. Beck, J. Appl. Phys. 40, 2269 (1969).

[76]H. Montgomery, G. P. Pells, and E. M. Wray, Proc. Roy. Soc. (London) A301, 261 (1967).

[77]P. M. Lee and P. E. Lewis, J. Phys. C 2, 1089 (1969).

[78]S. A. Ahern, M. J. C. Martin, and W. Sucksmith, Proc. Roy. Soc. (London) A248, 145 (1958).

[79]T. J. Hicks, B. Rainford, J. S. Kouvel, G. G. Low, and J. B. Comly, Phys. Rev. Letters 22, 531 (1969).